ELSEVIER

Deep-Sea Research II 52 (2005) 2990–3010

DEEP-SEA RESEARCH
PART II

www.elsevier.com/locate/dsr2

Satellite-derived spatial and temporal biological variability in the Cyprus Eddy

Steve Groom[a,*], Barak Herut[b], Steve Brenner[b,c], George Zodiatis[d], Stella Psarra[e], Nurit Kress[b], Michael D. Krom[f], Cliff S. Law[a,1], Panos Drakopoulos[d,g]

[a]*Plymouth Marine Laboratory, Prospect Place, Plymouth, PL1 3DH, UK*
[b]*National Institute of Oceanography, Israel Oceanographic and Limnological Research, P.O. Box 8030, Tel- Shikmona, Haifa 31080, Israel*
[c]*Department of Geography, Bar Ilan University, Ramat Gan 52900, Israel*
[d]*Oceanography Centre, Dept. of Fisheries & Marine Research, Nicosia, Cyprus*
[e]*Hellenic Center for Marine Research, P.O. Box 2214, 71003, Heraklion, Crete, Greece*
[f]*School of Earth Sciences & Earth and Biosphere Institute, Leeds University, Woodhouse Lane, Leeds LS2 9JT, UK*
[g]*Department of Optics, Technological Institute of Athens, Athens, Greece*

Received 8 March 2005; accepted 19 August 2005

Abstract

The cycling of phosphorus in the Mediterranean (CYCLOPS) team investigated phosphate limitation in the Eastern Mediterranean and conducted a phosphate addition experiment in 2002 at the centre of an anticyclonic eddy south of Cyprus. The 2002 and other cruises generated a small database of chlorophyll-a (chl-a) profiles that enabled investigation of the performance of a variety of standard and regional bio-optical algorithms for remote sensing retrievals of chl-a in the region. The standard SeaWiFS OC4V4 and MODIS chlor_a2 algorithms overestimated chl-a as previously reported while a regional algorithm proposed by Bricaud et al. [2002. Algal biomass and sea surface temperature in the Mediterranean basin: intercomparison of data from various satellite sensors, and implications for primary production estimates. Remote Sensing Environment 81, 163–178] and the semi-analytical MODIS chlor_a3 gave improved retrievals. SeaWiFS mean chl-a maps are presented for the Eastern Mediterranean for each month between September 1997 and August 2004 and as multi-annual "climatological" images. The former showed that chl-a in the region decreased over the duration of the time series with reductions in the centre of the eddy, tracked using a quasi-Lagrangian approach, of approximately 33% between 1997 and 1998 and 2002 and 2003. This was not correlated with deep winter mixing represented as heat loss from the sea-surface or dust deposition represented as daily EP-TOMS aerosol index and annual aluminium deposition on the Israeli coast. It is hypothesised that the variations in chl-a are partly a function of the eddy dynamics. Daily SeaWiFS observations show that the 2002 phosphate release was conducted at a period of decreasing chl-a between the winter maximum and summer oligotrophic conditions; however, the rate of seasonal decrease was less than that observed in situ during the week following the phosphate release.
© 2005 Elsevier Ltd. All rights reserved.

Keywords: Remote sensing; Ocean colour; SeaWiFS; Phosphate addition; Chlorophyll-a; Cyprus Eddy

*Corresponding author. Tel.: +44 1752 633150; fax: +44 1752 633101.
E-mail address: sbg@pml.ac.uk (S. Groom).
[1]Present address: National Institute of Water and Atmospheric Research (NIWA), 301 Evans Bay Parade, Greta Point, P.O. Box 14-901, Kilbirnie, Wellington, New Zealand.

0967-0645/$ - see front matter © 2005 Elsevier Ltd. All rights reserved.
doi:10.1016/j.dsr2.2005.08.019

1. Introduction

The Mediterranean is a virtually enclosed sea with a reverse estuarine circulation, driven by the excess of evaporation in the basin, that results in fresh, nutrient-poor surface flow into the basin with saltier, nutrient-richer deeper water outflow through the straits of Gibraltar (Bethoux et al., 1992). The Eastern Mediterranean behaves in a similar manner, with surface inflow and deeper water outflow through the Straits of Sicily. This results in an west to east gradient of decreasing surface chlorophyll-a (chl-a) (Turley et al., 2000) that is readily seen from space (Antoine et al., 1995), with the Eastern Mediterranean Levantine waters exhibiting highly oligotrophic conditions.

The Eastern Mediterranean has anomalously high ratios of nitrate to phosphorus and has been suggested to be phosphate-limited (Krom et al., 1991). In order to investigate the ecosystem response to phosphate enrichment, the cycling of phosphorus in the Mediterranean (CYCLOPS) project was conducted, with support from the European Commission. The project involved sampling of biological, chemical and physical properties (see Krom et al., 2005; Psarra et al., 2005) prior to and during a phosphate addition experiment in May 2002. The experiment was located in an warm-core, semi-permanent anticyclonic eddy south of Cyprus (Fig. 1A,B) for reasons described in Krom et al. (2005). The eddy also was sampled frequently in situ between 2001 and 2003 in order to characterise temporal variability. Remote sensing enabled observation of surface chl-a to locate the eddy prior to the cruises, and to observe any biological responses during the addition experiment.

It has been well established that satellite retrievals of chl-a in the Mediterranean using standard bio-optical algorithms are anomalously high when compared to in situ measurements, notably in the ultra-oligotrophic waters in the eastern basin (e.g., Gitelson et al., 1996; Bricaud et al., 2002). Various mechanisms have been proposed for this including the aeolian deposition of desert dust, which affects the scattering and absorption properties and, hence, influences bio-optical algorithms (Claustre et al., 2002). A number of "regional" bio-optical algorithms have been proposed for chl-a retrieval in the Mediterranean including Gitelson et al. (1996) for application to the Coastal Zone Color Scanner and Bricaud et al. (2002) and D'Ortenzio et al. (2002) both for use with SeaWiFS. However, no consensus algorithm has yet been established, and algorithms appear to be least accurate at very low chl-a concentrations ($<0.04\,mg\,m^{-3}$) typical of waters in the CYCLOPS study area, partly because in situ observations are relatively sparse.

Results showing seasonal cycles of chl-a in the eastern basin based on these algorithms have been published in D'Ortenzio et al. (2003) and Bosc et al. (2004). Unfortunately, both papers covered the period Sept 1997 to, respectively, the mid or end of 2001, i.e. outside the main experimental period of CYCLOPS in 2002 and 2003. Furthermore, since they considered the whole eastern basin, the variability in southern Levantine waters of interest in CYCLOPS is difficult to see (e.g., see Figs. 6 and 7 in Bosc et al., 2004).

The aims, therefore, of this communication are first, to compare the in situ chl-a data obtained during CYCLOPS with ocean-colour retrievals using standard and various regional algorithms to quantify the applicability to the study region. Second, to compute the seasonal cycle of chl-a (and primary production) within and around the Cyprus Eddy for the period 1997–2004 and to present results in a form appropriate for these ultra-oligotrophic waters. Third, to investigate factors influencing the interannual variability in chl-a and to provide the *natural* context within which any induced response may be observed. Finally, to show the daily variability in the eddy before, during and after the enrichment experiment, and to investigate whether any change in chl-a concentration is observed from space.

2. Methods

2.1. In situ chl-a estimates

During CYCLOPS chl-a was measured on a number of cruises (RV Aegaeo: April 2001, May 2001, March 2002 and May 2002; RV Shikmona: January 2003 and May 2003) using fluorometry (Yentsch and Menzel, 1963) following the methods described in detail in Psarra et al. (2005). On the phosphate addition experiment in May 2002, high-performance liquid chromatography (HPLC: Mantoura and Llewellyn, 1983) was employed for chl-a and accessory pigment determination in addition to fluorometry. However, for consistency, only the fluorometrically determined chl-a were used. For comparison with satellite retrievals it is necessary to estimate the chl-a that would be "seen" by the

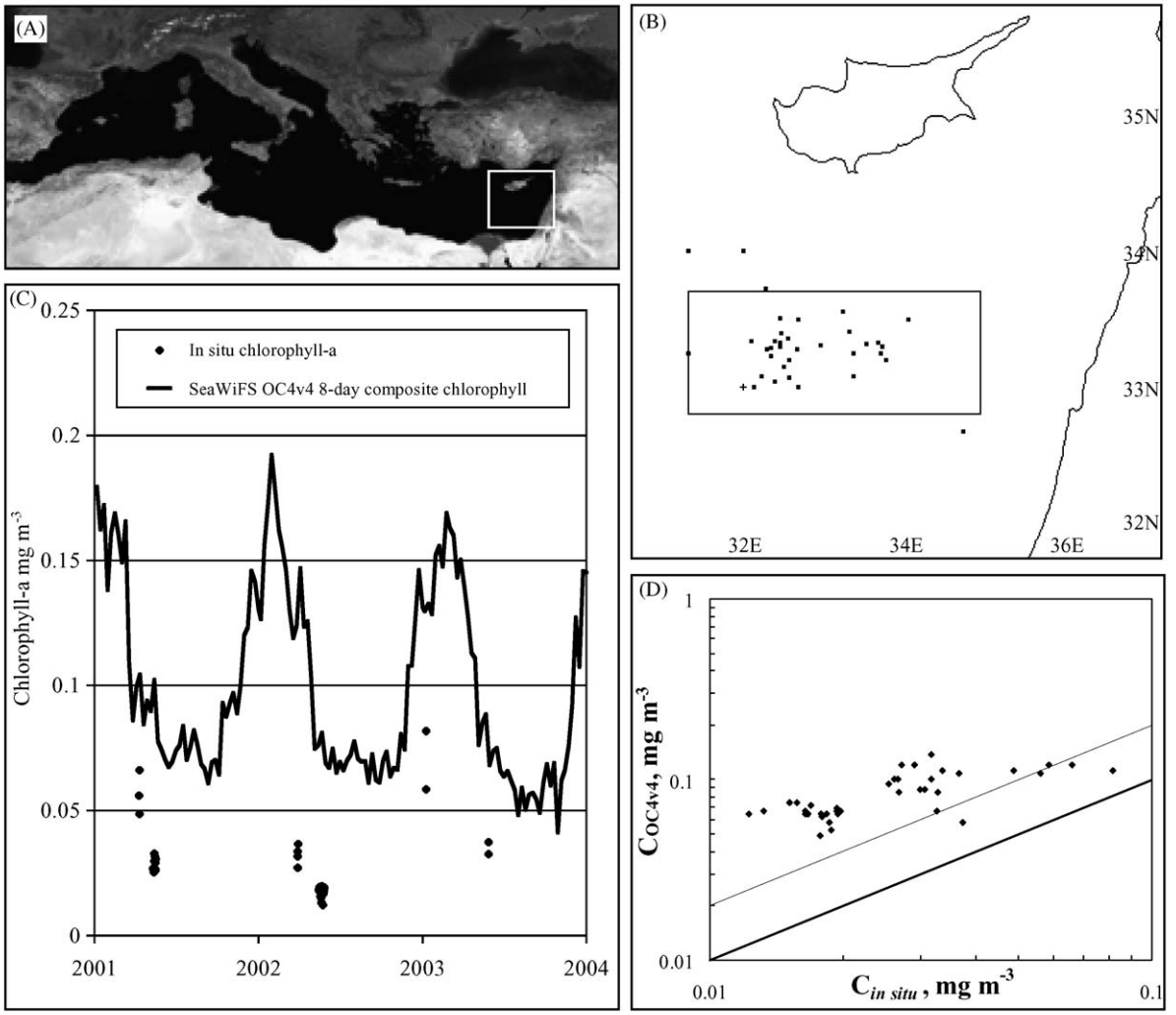

Fig. 1. (A) A satellite view of the Mediterranean Sea showing the study region south of Cyprus; (B) a map of the study region with location of in situ chl-a profiles used for the SeaWiFS validation; (C) comparison of SeaWiFS 8-day chl-a estimates using the OC4v4 algorithm and in situ chl-a, 2001–2003; (D) data from c re-plotted as a regression. Note log scales; parallel lines indicate the 1:1 and 2:1 lines.

satellite (Gordon and Clark, 1980). This is particularly important when there are strong near-surface gradients, though it should be stressed that the area of this study generally has weak near-surface gradients. The satellite-sensed chl-a (C_{sat}) is the optically weighted chl-a for the first penetration depth:

$$C_{sat} = \frac{\int_0^{Zpd} C(z)\exp\{-2kz\}\,dz}{\int_0^{Zpd}\exp\{-2kz\}\,dz},$$

where the weighting function is the attenuation of light from the surface to depth z (m) and back to the surface, and k (m^{-1}) is the attenuation coefficient of broadband irradiance. Values of C_{sat} were computed using the in situ chl-a profiles and an estimate of k based on chl-a (Morel and Berthon, 1989). Chl-a measurements taken close to the coast were excluded since the satellite data are likely to be affected by the presence of coloured dissolved organic matter or suspended particulate matter (e.g., Karabashev et al., 2002).

2.2. Satellite data

Ocean colour data were obtained from two sensors, the Sea-viewing Wide Field-of-view Sensor (SeaWiFS: McClain et al., 2004) and the Moderate

Resolution Imaging Spectroradiometer (MODIS: Esaias et al., 1998). SeaWiFS began observation of ocean colour in September 1997, providing measurements at ~1.1 km resolution at nadir in six bands in the visible and two in the near-infra-red. The visible bands were chosen in regions of high, medium and low chl-a absorption (O'Reilly et al., 1998). During the CYCLOPS cruises data were obtained in near-real time as mapped "level2" (chl-a product) images and were used as a guide for in situ sampling. Subsequent to the project daily SeaWiFS "reprocessing 4" data were obtained in unmapped level-1 and level-2 format at full-resolution from the NASA Ocean Color web site (http://oceancolor.gsfc.nasa.gov/) for the period September 1997 to August 2004. Images were re-mapped to common geographical projection following Lavender and Groom (1999). These comprised ~2800 passes and enabled daily observation of ocean-colour variability over the study region limited by cloud-cover and satellite viewing geometry. Images were produced showing either purely cloud-free pixels or with pixels masked where any of the 24 quality "flags" were set (Baith et al., 2001). The quality flags mark any potential sources of erroneous measured reflectance or retrieved chl-a values. Chl-a was computed using NASA standard global bio-optical algorithm OC4v4, the latest version of the four-band switching algorithm (O'Reilly et al., 1998) where

$$\text{Chl-a} = 10^{(0.366-3.607R+1.930R^2+0.649R^3-1.532R^4)},$$

where R is the logarithm of the maximum ratio out of $R_{rs}^{443}/R_{rs}^{555}$, $R_{rs}^{490}/R_{rs}^{555}$, or $R_{rs}^{510}/R_{rs}^{555}$, and R_{rs}^{λ} is the remote sensing reflectance for SeaWiFS band λ (see O'Reilly et al., 1998).

Chl-a also was computed using the region specific algorithms of Bricaud et al. (2002) from the $R_{rs}^{443}/R_{rs}^{555}$ ratio and D'Ortenzio et al. (2002) from the $R_{rs}^{490}/R_{rs}^{555}$ ratio. In SeaWiFS reprocessing 4 it is valid to use inputs of R_{rs} from the standard processing level-2 files to compute chl-a, in contrast to reprocessing 3 where, as noted by D'Ortenzio et al. (2002), the retrieved R_{rs} values depend on the interim chl-a estimate which is calculated using OC4v4. In reprocessing 3 the Siegel et al. (2000) iterative near-infra-red correction was applied even at very low chl-a concentrations; in reprocessing 4 at chl-a concentration $<0.3\,\mathrm{mg\,m^{-3}}$ no correction is applied.

SeaWiFS "9 km" composite data also were obtained from the Goddard GES Distributed Active Archive Center (http://daac.gsfc.nasa.gov/data/dataset/SEAWIFS/index.html) at daily, 8-day and monthly resolution. The composite data provide abstraction at lower spatial or temporal resolution and include all data that pass the SeaWiFS quality flags (Baith et al., 2001). These data were used for observation of large-area spatio-temporal variability and for computation of primary production.

MODIS on board the Terra spacecraft was launched in 1999 and provides ocean colour observations at similar resolution to SeaWiFS (~1 km) but with more bands. Note that no situ/satellite comparisons were possible with the more recent MODIS/Aqua instrument. Terra/MODIS data were obtained as level-2 (geophysical and biological products) from the Goddard-DAAC solely for comparison with in situ chl-a values. A variety of chl-a algorithms are employed with MODIS: chlor_a2 utilises a band switching algorithm with three MODIS bands (OC3: O'Reilly et al., 1998) and is, therefore, analogous to SeaWiFS OC4v4, and chlor_a3 uses the semi-analytical case-2 chl-a algorithm of Carder et al. (1999).

2.3. Satellite—in situ matchups

In order to evaluate satellite chl-a algorithms by comparison with in situ data, strict criteria were used to ensure the quality of the former: satellite data were from the same day as the in situ measurements; none of the 24 SeaWiFS quality flags (or the MODIS flags) were set for the pixels under comparison; and only full resolution 1-km data were used (D'Ortenzio et al., 2002; McClain et al., 2004).

2.4. In situ estimates of SF_6

As described in Law et al. (2005), the movement of the water containing the added phosphate in the May 2002 cruise was marked using SF_6 tracer. In order to compare satellite derived estimates of chl-a inside and outside the patch, an operational background of $3\,\mathrm{fmol\,l^{-1}}$ SF_6 was used as the threshold (see Law et al., 2005 for more details).

2.5. Satellite estimates of primary production

Estimates of phytoplankton primary production (PP) using satellite data as inputs were computed following essentially the same method as Joint et al.

(2002) using the model of Morel (1991):

$$\mathrm{PP} = 12 a^*_{\max} \varphi_{\mu,\max} \int_{\text{sunrise}}^{\text{sunset}} \int_0^{z_{0.1\%}} \int_{400}^{700} C(z)\mathrm{PUR}(z,t,\lambda) \times f(x(z,t))\, \mathrm{d}\lambda\, \mathrm{d}z\, \mathrm{d}t,$$

where $a^*_{\max}$ (m^{-1} (mg Chl m^{-3})$^{-1}$) is the maximum value of the chl-a-specific phytoplankton absorption spectrum and $\varphi_{\mu,\max}$ (mole Carbon (mol photons absorbed)$^{-1}$) is the quantum yield for growth; $C(z)$ is the chl-a concentration (mg m^{-3}) at depth z; PUR (W m^{-2} nm^{-1}) at depth z, time t and wavelength λ, is the photosynthetically usable radiation (spectral photosynthetically active radiation weighted by the spectral phytoplankton absorption); f is a function that relates carbon production to total usable light at depth z and time t expressed as a dimensionless parameter x equal to PUR/KPUR. The irradiance scaling factor (KPUR) was set to 80 μmol quanta m^{-2} s^{-1} at 20 °C (Morel et al., 1996) and varied with temperature, T (°C), according to $\mathrm{KPUR}(T) = \mathrm{KPUR}(20)1.065^{(T-20)}$. Following Morel et al. (1996), $\varphi_{\mu,\max}$ and $a^*_{\max}$ were parameterised as a function of chl-a concentration. The integration was performed over all daylight hours, for wavelengths 400–700 nm and to the productive depth, $Z_{0.1\%}$, which is defined here as the 0.1% light level and computed through the iterative approach of Morel and Berthon (1989). The model has been parameterised against 24-h in situ incubations and, hence, retrieves net primary production.

The model was forced with daily satellite-derived estimates of chl-a and sea-surface temperature and irradiance computed from Gregg and Carder (1990), with input meteorological variables from National Center for Environmental Prediction (NCEP) reanalysis fields, and cloud cover from the European Centre for Medium-range Weather Forecasting (ECMWF). Where no valid satellite chl-a or SST data were available the last valid data were used. Vertical profiles of chl-a were computed from SeaWiFS C_{sat} values following the method of Morel and Berthon (1989) modified to ensure that the retrieved C_{sat} value equalled the initial specified C_{sat} value. Following Bosc et al. (2004) where the euphotic depth (1% light level) was found to be shallower than the mixed layer given by Levitus (1982) the chl-a was assumed to be constant with depth. This is the case during deep mixing in February–March. Vertical temperature profiles were constructed following a similar method to Bricaud et al. (2002): surface temperature was extracted from Reynolds SST (Reynolds and Smith, 1995) fields and combined with the Levitus climatological vertical profiles for that location. Where Levitus gave different surface values the mixed layer was set equal to the Reynolds value.

3. Results and discussion

3.1. In situ chl-a data

Application of the in situ acceptance criteria mentioned in the previous section resulted in a total of 43 vertical profiles of chl-a at locations shown in Fig. 1B. Vertical profiles showed deep chlorophyll maxima at 130–140 m (data not shown) deeper than previously reported by Yacobi et al. (1994) and Zohary et al. (1998) for the same region but at other times of the year. C_{sat} values varied from ~0.01 to 0.08 mg m^{-3} (Fig. 1C, D), with highest values in January 2003 and April 2001 and lowest in May 2002 when the chl-a was between 0.01 and 0.02 mg m^{-3}. These results are in accordance with previous observations on the extreme oligotrophic nature of the Eastern Mediterranean (e.g., Berman et al., 1984). The in situ C_{sat} values are regressed against SeaWiFS 8-day, 9-km composite values in Fig. 1D. It should be stressed that this comparison is between an individual in situ chl-a datum with a 9.8-km × 8.2-km, 8-day C_{sat} mean, and so spatial and temporal variability will contribute to satellite-in situ differences. Nevertheless, Fig. 1D shows that standard SeaWiFS OC4v4 satellite retrievals were consistently above the in situ values as previously observed in the Mediterranean (Bricaud et al., 2002; D'Ortenzio et al., 2002; Bosc et al., 2004) and in the Eastern Mediterranean in particular (Gitelson et al., 1996).

A comparison of the in situ measurements and satellite retrievals revealed only 13 SeaWiFS and 12 Terra/MODIS match-ups that passed all the satellite criteria noted in the methods; however, the value in these data is that they are predominantly in the ultra-oligotrophic 0.01–0.02 mg m^{-3} range, and are concentrated in one small area. This range contrasts with the data presented in D'Ortenzio et al. (2002), where chl-a were >0.05 mg m^{-3}, and in Bricaud et al. (2002), where chl-a was >0.03 mg m^{-3}. Furthermore, the NASA SeaWiFS in situ—satellite match-ups are notably sparse in the very low chl-a range (see McClain et al., 2004). Hence, although the data set is too small to either construct a region-specific

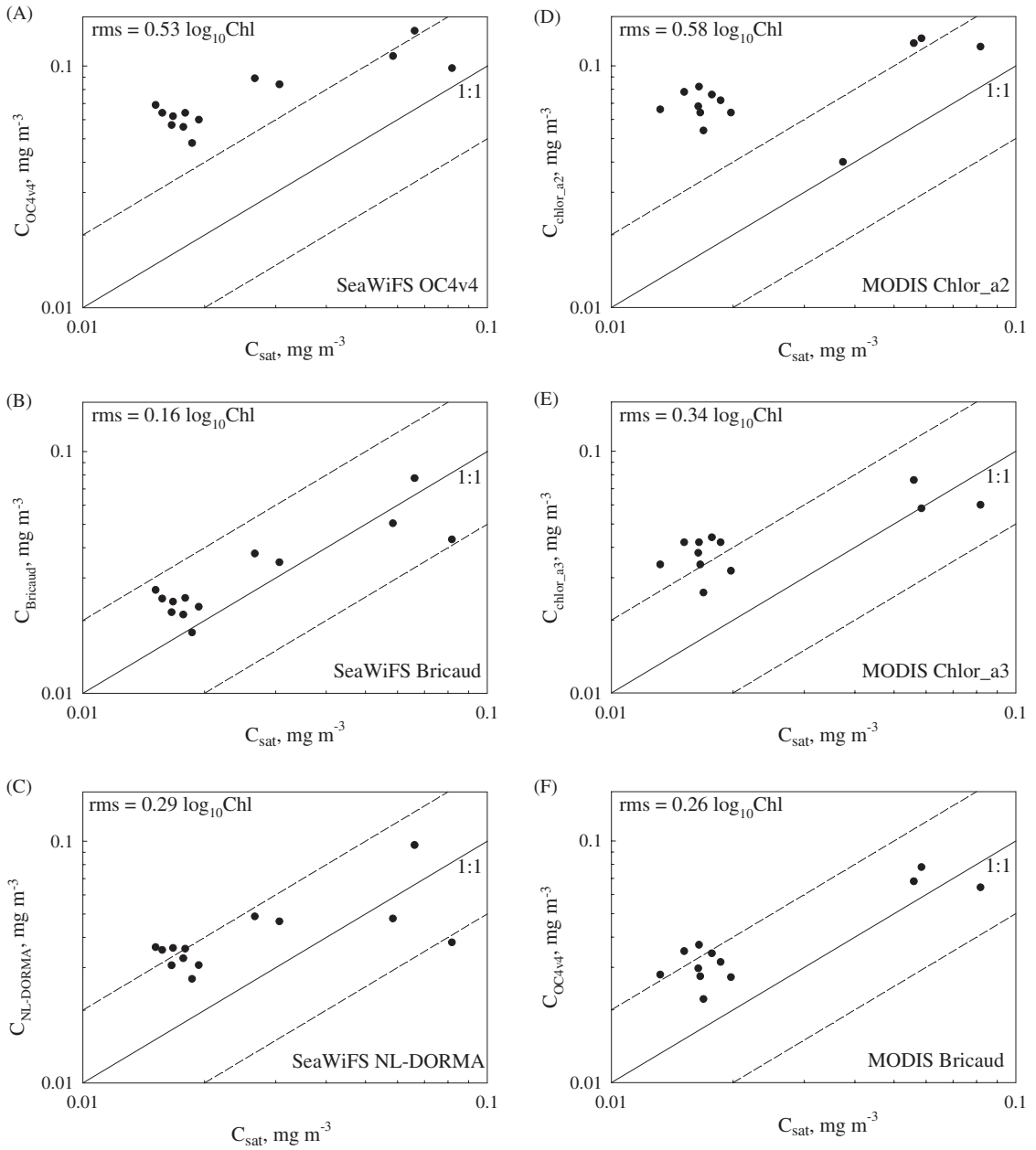

Fig. 2. SeaWiFS and MODIS matchups: SeaWiFS retrievals compared to in situ C_{sat} for (A) OC4v4; (B) Bricaud et al. (2002) and (C) D'Ortenzio et al. (2002) NL-DORMA algorithms. MODIS retrievals compared to in situ C_{sat} for (D) MODIS chlor_a_2, (E) chlor_a_3 and (F) Bricaud et al. (2002) algorithms.

algorithm or adjudicate on the relative merits of a particular algorithm for the Mediterranean Sea, in general it does enable evaluation of the performance of algorithms for this specific environment.

Fig. 2 shows the comparison of in situ C_{sat} values with a number of SeaWiFS and MODIS algorithms. In each case the root-mean-square error (RMSE) is calculated with respect to the 1:1 line to give a measure of the closeness of fit of the satellite retrievals to the in situ data. The SeaWiFS standard OC4v4 algorithm (Fig. 2A) overestimated chl-a, notably in the 0.01–0.02 mg m^{-3} range by a factor of 5 to 6, with most points outside the 2:1 line and RMSE = 0.53 $\log_{10}$ Chl-a. By comparison two recent Mediterranean-specific algorithms improved chl-a retrievals (Fig. 2B, C): the Bricaud et al.

(2002) algorithm (hereafter B2002) gave RMSE $\sim$0.16 $\log_{10}$ Chl-a and the D'Ortenzio et al. (2002) non-linear algorithm gave RMSE $\sim$0.29 $\log_{10}$ Chl-a. Both algorithms overestimated the lowest chl-a values, but in the case of B2002 this factor is $\sim$33% in the 0.01–0.02 mg m^{-3} range. It should be stressed that the comparison of in situ chl-a with satellite retrievals is a test of the entire satellite system, including the calibration, bio-optical algorithm and atmospheric correction (though as noted by D'Ortenzio et al., 2002, the SeaWiFS criteria exclude anomalous atmospheric conditions and so these are not explicitly tested). These results compare favourably with NASA SeaWiFS match-up comparisons where the RMSE $\sim$0.24 $\log_{10}$ Chl-a with respect to the regression line and over a much wider range of chl-a ($\sim$0.03–30 mg m^{-3}).

Fig. 2D–F shows the MODIS retrievals: the SeaWiFS analogue chlor_a2 algorithm overestimated chl-a with a similar RMSE (0.58 $\log_{10}$ Chl-a) to SeaWiFS OC4v4. This is expected since both are band-switching algorithms (O'Reilly et al., 1998) that for the CYCLOPS region have maximum R_{rs} ratios of $R_{rs}^{443}/R_{rs}^{555}$ and $R_{rs}^{443}/R_{rs}^{551}$ for MODIS. The MODIS case-2 algorithm (chlor_a3: Carder et al., 1999) gave lower RMSE ($\sim$0.34 $\log_{10}$ Chl-a), suggesting that the semi-analytical approach of this algorithm may be less affected by factors that give erroneous ocean-colour retrievals in the Mediterranean: however, such conclusions must await more comprehensive calibration studies. Finally, MODIS data have been used with B2002: since this requires R_{rs} at 555 nm the MODIS 551 nm band data have been reduced by 5%, representing the difference between monochromatic water leaving radiance at these two wavelengths (Gerald Moore, PML: pers. comm.). The resulting retrievals gave a significant improvement on chlora_2 with a lower RMSE $\sim$0.26 $\log_{10}$ Chl-a, but the lower range of chl-a values are still too high. This poorer performance may be a result of residual problems with the MODIS on the Terra spacecraft (as opposed to the more recent MODIS on the Aqua platform).

The SeaWiFS retrievals presented herein have used the B2002 algorithm: in doing so it is not suggested that this algorithm is the "best" for the Eastern Mediterranean, merely that it gave better results when compared with a small, regionally focused dataset obtained in CYCLOPS. Application of the B2002 algorithm to the SeaWiFS 8-day composite images used in Fig. 1D gave improved retrievals when compared to in situ data, of $\sim$0.2 $\log_{10}$ Chl-a (data not shown) compared to 0.54 $\log_{10}$ Chl-a in Fig. 1C. The remaining error in chl-a retrievals with B2002 is a function of chl-a with larger overestimation ($C_{\mathrm{SeaWiFS}}/C_{\mathrm{in\,situ}} = 1.51$, SD = 0.39, $n = 34$) at the lower chl-a $\sim$0.02–0.04 mg m^{-3} typically found between May and November (see Fig. 5) and lower errors ($C_{\mathrm{SeaWiFS}}/C_{\mathrm{in\,situ}} = 0.92$, SD = 0.17, $n = 5$) at chl-a values >0.05 mg m^{-3} found in other months. Hence, a simple improvement could be to arbitrarily divide B2002 chl-a values <0.05 mg m^{-3} by 1.5 and comparison with in situ values gives a RMSE of $\sim$0.12 $\log_{10}$ Chl-a. This is not used in the following analysis but is briefly discussed in terms of influence on primary production below.

3.2. Seasonal distributions of surface chl-a in the Levantine Basin

Mean monthly surface B2002 chl-a distributions were calculated from monthly SeaWiFS R_{rs} data from September 1997 to August 2004 and presented in Fig. 3. The values are similar to those in D'Ortenzio et al. (2003) using the DORMA algorithm for the period September 1997 to early May 2001, but the scaling in the latter was appropriate to the whole of the Eastern Mediterranean and showed little variability in the Levantine for many months. The data in Fig. 3, not surprisingly, agreed well with the chl-a maps for 1999 presented in Bosc et al. (2004) who also used the B2002 algorithm.

The wider spatial and temporal variability in the Levantine previously has been described by a number of authors including Antoine et al. (1995), D'Ortenzio et al. (2003), and Bosc et al. (2004), and is only briefly considered herein. The north-south gradient in chl-a concentrations is apparent in most months, with the lowest values found in the south during June to September and highest values in the north in January–February. The most prominent mesoscale features are the Rhodes Gyre, seen as elevated chl-a southeast of Rhodes for much of the year (studied in detail by D'Ortenzio et al., 2003) and in the south the low chl-a cores of the Shikmona (Cyprus) Eddy and Mersah Metru gyres (Ozsoy et al., 1993). Elevated chl-a values are apparent along the Egyptian, Israeli and Lebanese coasts, but these are probably affected by the presence of coloured dissolved organic matter (CDOM) and/or suspended particulate matter (SPM) in these coastal waters that influence the water optical properties and the water leaving signal

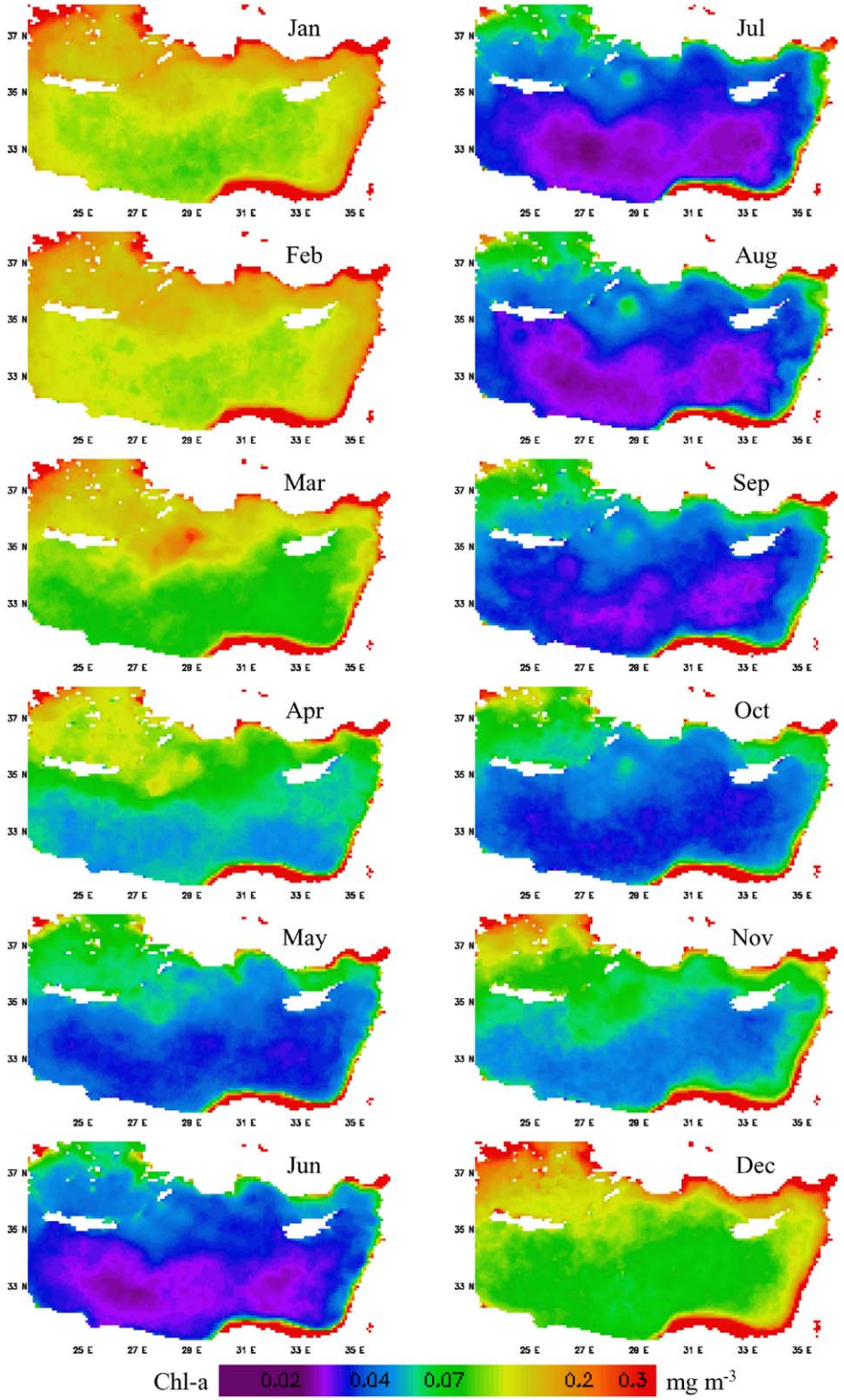

Fig. 3. Multi-annual or "Climatological" monthly mean SeaWiFS chl-a maps calculated using the B2002 algorithm. Note that the colour scale is logarithmic.

(e.g., Prieur and Sathyendranath, 1981). The filaments apparent in the seven-year averages (e.g., in March and August) as plumes of higher chl-a extending from the Israeli and Lebanese coasts suggest the regular seasonal appearance of these mesoscale features. In a series of high-resolution numerical simulations of the circulation in the south-eastern Levantine Basin, Brenner (2003) found that even for conditions of climatological forcing, filaments and eddies often form along the shelf/slope jet flowing along the coasts of Israel and Lebanon, and, in the upper layers, transport shelf water into the open sea. These features generally move westward or north-westward and maintain their signal for as much as several hundred kilometres before mixing with the open-sea water and thereby dissipating. This agrees well with the seven-year average chl-a distributions in the eastern Levantine as shown in Fig. 3 as well as with the maps showing the inter-annual variability in the next section. These filaments and eddies can occur in all seasons but are more noticeable in summer.

3.3. *Inter-annual variability in chl-a in the CYCLOPS study area*

The interannual variability in the CYCLOPS study area and the Cyprus Eddy is shown in Fig. 4, comprising individual SeaWiFS monthly chl-a extracts south of Cyprus. The images are ordered from September in one year to August the following year as opposed to a calendar year, which would split the chl-a maximum between two years. In situ observations of eddy locations are shown on Fig. 4, with a large black circle denoting the "principal" eddy, smaller black circles denoting "secondary" eddies (Zodiatis et al., 2001, 2002, 2004, unpublished data) and large white circles noting the CYCLOPS May 2001 and May 2002 study areas (Zodiatis et al., 2005). It is clear from both the satellite and in situ data that the Cyprus Eddy moved westward throughout the period, and a secondary anticyclonic eddy was observed to the east of the Cyprus Eddy from late 2002 to 2003 during the Cyprus Basin Oceanography (CYBO) cruises. In 2004, the flow pattern of the area during the CYBO cruises showed a single, well-developed, anticyclonic eddy south of Cyprus, together with the eastward meandering Mid-Mediterranean jet (MMJ: Zodiatis, unpublished data).

In Fig. 4 chl-a concentrations are low in September and October at $\sim$0.025–0.035 mg m^{-3}, with a slight increase in November, followed by a widespread increase in December to >0.1 mg m^{-3}. Elevated levels are present in January and February with reduction in March, with the exception of 1998, 2000 and 2003 when higher levels persisted. By May each year the summer oligotrophic conditions have become established with values similar to September. The Cyprus Eddy is manifested as a distinct lower chl-a region for most of May to October, with the exception of July–August 2001 when little surface signature was apparent. A small, low chl-a core first appears in May, notably in 2002 and 2003, and then extends in width during later months. During summer high-chl-a filaments from the Israeli coast frequently become entrained in the outer boundary of the anticyclonic eddy (e.g., July–September 1998 and August–October 2000): this also has the effect of more clearly defining the eddy centre, and is particularly clear on individual daily satellite passes (data not shown). The influence of the coastal filaments undoubtedly leads to higher average chl-a when computing statistics for larger-scale regions. As noted above, such features have been found in high-resolution model simulations of this region. It is quite clear that these filaments and eddies play a central role in transporting the chl-a rich shelf water into the open sea, especially in summer (Karabashev et al., 2002).

To complement these images, a time plot of monthly average chl-a was computed to observe change in chl-a in the eddy centre as it moved westward. A quasi-Lagrangian approach was used whereby the mean location of the eddy centre from the in situ observations was computed for each year and satellite chl-a data extracted within a box $\pm 0.3^{\circ}$ latitude and $\pm 0.4^{\circ}$ longitude centred on this position.

A striking feature in Fig. 4 is the progressively lower chl-a between 1997 and 2004 over the whole area. Since the images are presented as log-transformed data, the reduction is most noticeable at low chl-a between June and November whereas Fig. 5A shows that a reduction is also observed in winter. October, and notably November, exhibit significant reductions, with chlorophyll halving from $\sim$0.06 mg m^{-3} in 1997 to $\sim$0.03 mg m^{-3} in 2003. The eddy centre chl-a (Fig. 5A) shows clear reductions between 1997–1998 and 2002–2003, with the yearly maximum decreasing from $\sim$0.145 to 0.091 mg m^{-3} (a reduction of 37%), minimum from 0.027 to 0.018 mg m^{-3} (33%) and the average chl-a from 0.066 to 0.044 mg m^{-3} (33%). For compar-

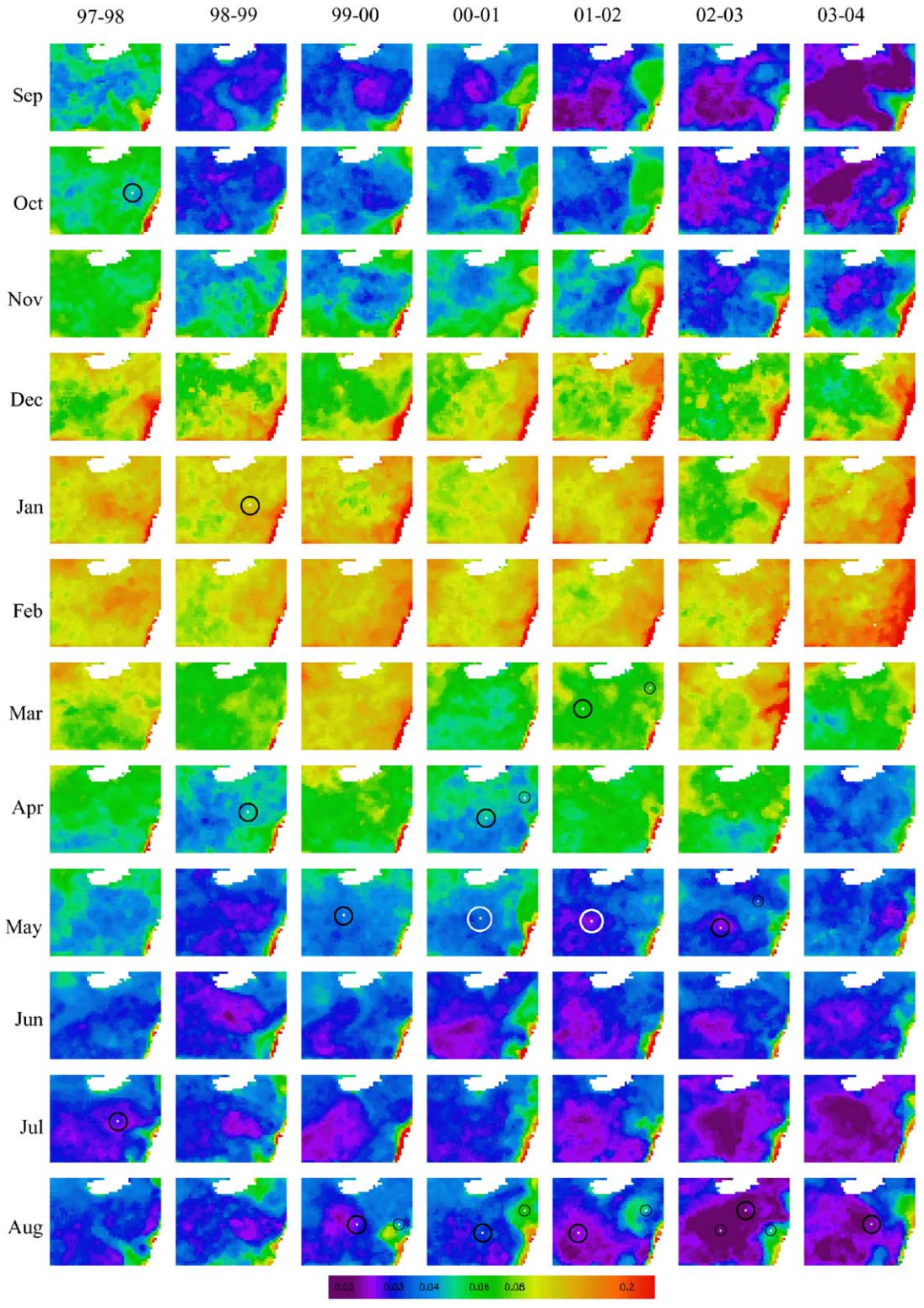

Fig. 4. Individual monthly chl-a maps using the B2002 algorithms with overlaid eddy centre locations determined from in situ observations: large black circle "main" Cyprus Eddy; small black circle, "secondary" eddies; large white circle, CYCLOPS cruises in May 2001 and 2002.

ison, average monthly chl-a was extracted for two further regions within the oligotrophic region in the south Levantine but outside the direct influence of the Cyprus Eddy (located at 33–34°N 29.5–30.5°E and 33–34°N and 26–27°E) and farther from the higher chl-a filaments off the Israeli coast. The chl-a values for the two western regions (Fig. 5B, C) are comparable in magnitude to the eddy centre, but, in contrast, show no evidence for systematic reductions over time; indeed, the westernmost region shows evidence of an increase in annual maxima over the period. This suggests that the temporal changes are predominantly associated with the dynamics of the eddy, though it should be noted that the eddy periphery also shows reductions with time (e.g., compare August and September images between years on Fig. 4).

The primary nutrients sources driving chl-a in the eddy, assuming isolation from the coastal jets, are winter deep-water mixing and airborne deposition (Herut et al., 2002). Hence, in order to investigate possible factors responsible for this variability, a variety of forcing variables were examined. D'Ortenzio et al. (2003) showed how the chl-a variability in some regions of the Eastern Mediterranean, such as the Rhodes Gyre, is well correlated with the net heat flux that forces winter convection, mixing deeper nutrients into the water column (Stratford and Haines, 2002). The implication of such a correlation is that the dominant process that controls the bloom is the one-dimensional deep vertical mixing in winter that brings nutrients from deeper waters as the seasonal thermocline is eroded. This will have an immediate effect on the bloom, indeed, as noted in Zohary et al. (1998) and Krom et al. (2003a), the bloom coincides with the period of maximum vertical mixing; however, it is not clear whether the system has a long enough memory for the summer conditions to be affected by mixing during the previous winter. Conditions also will depend on the relative importance of horizontal advection above the seasonal thermocline in summer. Following D'Ortenzio et al. (2003) daily estimates of the net heat flux (a sum of the latent, sensible, longwave and short-wave fluxes) were computed from the US National Center for Environmental Prediction (NCEP: http://www.cdc.noaa.gov/cdc/reanalysis/reanalysis.shtml) reanalyses and shown in Fig. 6A. Not surprisingly the heat fluxes for 1998–2001 are similar to those shown in D'Ortenzio et al. (2003); however, there is no visual correlation in the heat flux and the chl-a reductions observed in the eddy centre (Fig. 5A). Conversely, the relative chl-a trends in the two western regions (Fig. 5b, C) do partially correlate with the heat flux, generally increasing between 1997–1998 and 1999–2001 decreasing in 2001–2002 and increasing again in 2002–2003. D'Ortenzio et al. (2003) found no correlation between chl-a and heat flux in the eastern Ionian Sea and proposed the dynamic structure of the water as a factor in the onset of blooms.

The influence of the heat flux on the chl-a concentration inside and outside the Cyprus Eddy possibly can be explained as follows: the winter convective cooling initiated by heat loss at the surface will cause mixing to a given depth dependent on the magnitude of the heat loss. Observations of the Cyprus Eddy (e.g. Zodiatis et al., 2005) show the characteristic depression of the isotherms in this warm-core eddy, and Zodiatis et al. (2001) observed mixing to 350 m in 2000. Krom et al. (1993) noted that in February 1989 the nutricline was 450–700 m at the eddy core and 200–450 m and the boundary (though it should be stressed that this was a different, possibly more intense Cyprus Eddy: Krom, unpublished data). During severe weather conditions in the Eastern Mediterranean Levantine Basin, such as in 1987, the winter convective mixing penetrated to 1000 m, deeper than observed in 1999–2000 in the frame of MFSPP project (Zodiatis, unpubl. observations). Hence, it is suggested that within the eddy, in many years, the winter convection may not penetrate to the deeper nutrient richer waters and, therefore, mixing only brings limited additional nutrients into the eddy core. The only new nutrients supplied to the eddy core thus come from atmospheric (mainly dust) input. Conversely, outside the eddy the shallower nutricline permits higher nutrient input to the mixed layer as well as supply by horizontal advection including supply from coastal filaments. These data suggest that the input from atmospheric sources to the eddy core is less than the flux of nutrients lost from the system by vertical export. Such a process is consistent with the results from Brenner (1993) where it was shown that the water in the core of the eddy (mixed layer in winter and thermostad in summer) could retain its identity for a period of several years until some change in the circulation causes a reset of the system. The dynamical processes that lead to such a reset are most likely a combination of deep winter mixing and horizontal advection. The higher chl-a

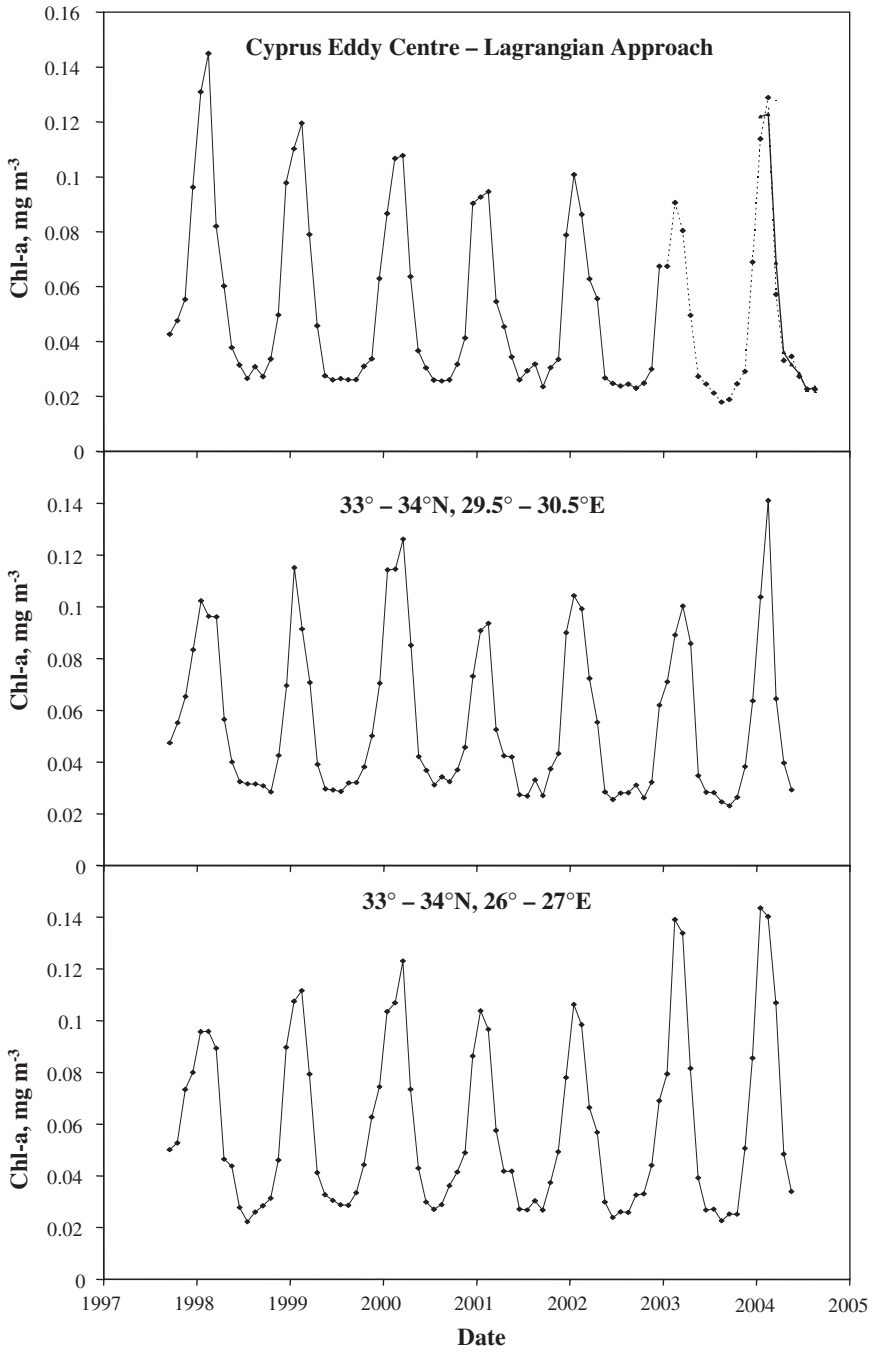

Fig. 5. (A) Mean monthly SeaWiFS chlorophyll variations in (A) the eddy centre calculated using the Bricaud et al. (2002) regional algorithm. The dotted line shows chlorophyll at the location of the old eddy while the solid line in 2004 refers to the secondary or new eddy centre (see text for details); (B) and (C) mean monthly SeaWiFS chl-a variations in two boxes outside influence of Cyprus Eddy calculated using the Bricaud et al. (2002) regional algorithm.

values in winter 2003–2004 may be explained by more significant changes in the dynamics of the regions (Zodiatis et al., 2005; Zodiatis unpublished observations) since the "old" eddy was not detected from in situ sampling in the region in 2004.

Since atmospheric deposition is probably the main source of new production in the eddy (Herut

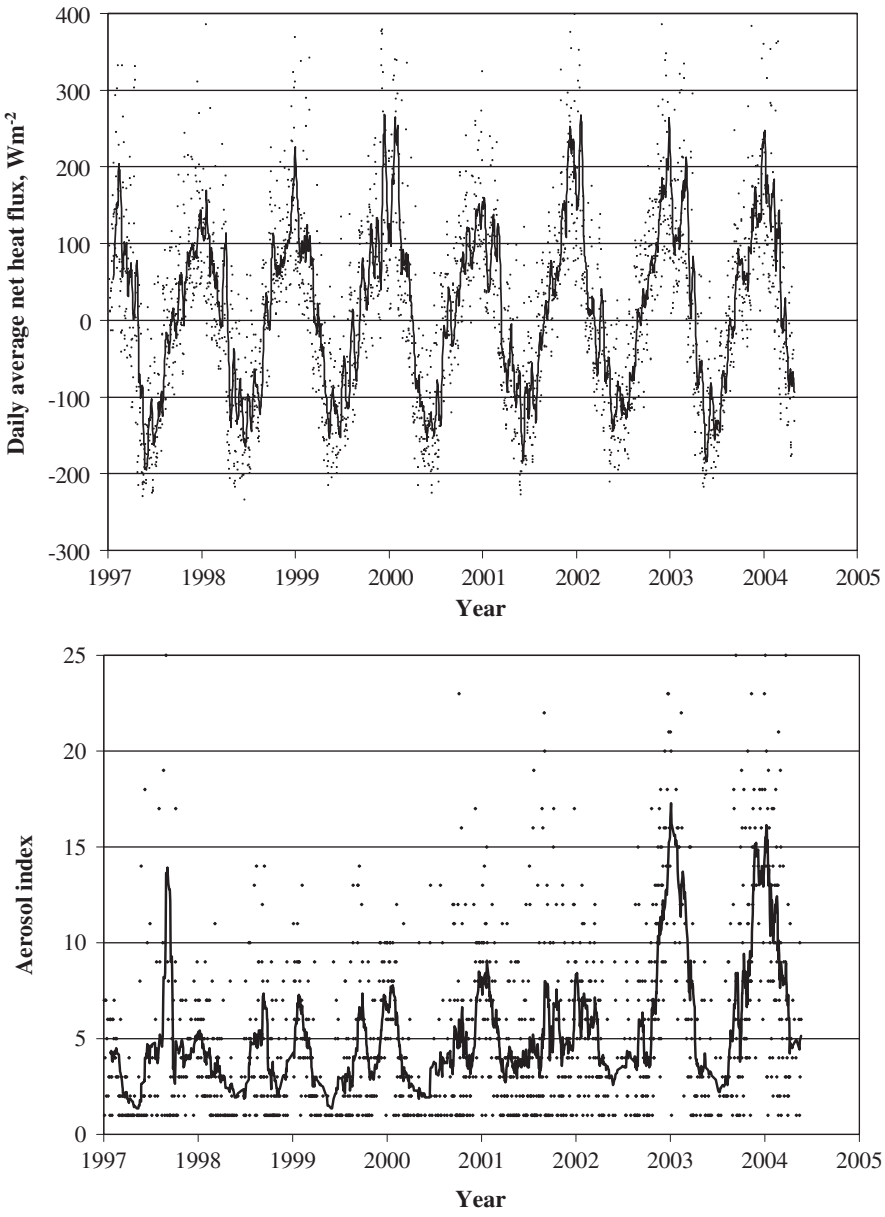

Fig. 6. (A) NCEP reanalysis daily average net heat flux (sensible + latent + longwave + shortwave) with 15-day running mean at 33 N 33E; (B) EP-TOMS absorbing aerosol index with 14-day running mean.

et al., 1999; Krom et al., 2003b) two measures of aerosols over the Eastern Mediterranean were investigated. First, daily absorbing aerosol index (AI) derived from the earth probe total ozone mapping system (EP-TOMS: Hsu et al., 1996) were obtained for 1997 to mid-2004 and plotted in Fig. 6B. The AI gives a measure of absorbing aerosols that in this region are related to Saharan dust. Second, the annual variability of Al flux measured at Tel-Shikmona on the Israeli coast from 1996 to 2003 (Herut et al., 2004) was used as proxy of dust deposition variability over the eddy (Fig. 7). There is no positive correlation with the chl-a variability observed in Fig. 5A–C, but there is a distinct increase in the AI in 2002–2003 and 2003–2004 over the whole region. The Al flux also shows a general increase between 1996 and 2003 with a notable minimum in 1999. It is interesting to speculate that if the increase in AI and Tel-Shikmona Al depositions, as evidenced in Figs. 6B and 7, represent an

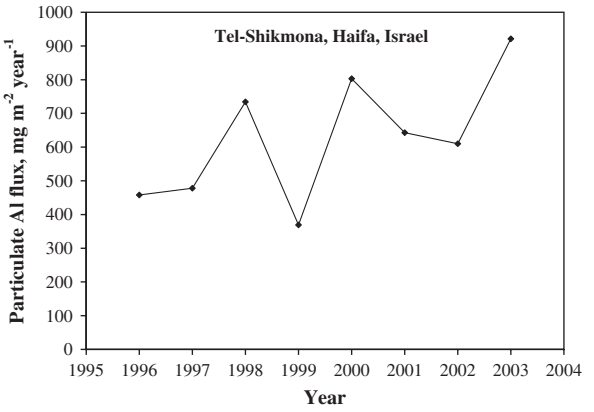

Fig. 7. Atmospheric fluxes of particulate Al at Tel-Shikmona (Haifa, Israel) during 1996–2003. Annual fluxes were calculated on the basis of sampling during ~25% of the total annual days.

Table 1
Inter-annual variation of integrated primary production computed from September to August the following year

Yearly cycle	PP gC m^{-2} year^{-1}
1997–1998	84.2
1998–1999	70.4
1999–2000	69.7
2000–2001	69.4
2001–2002	63.3
2002–2003	63.7
2003–2004	64.5

increase in dust deposition and atmospheric nutrient input to surface waters (Herut et al., 2002) then why is there not an increase in chl-a? It may be that there are competing processes of which dust deposition is of lesser importance, whereas if dust had a major positive (or negative) impact on chlorophyll concentrations it would be reasonable to expect similar increases (or decreases) across the entire Eastern Mediterranean.

As noted above, it is also possible that filaments and eddies transport chl-a-rich water from the shelf into the Cyprus Eddy region and affect the chl-a concentrations. In order to assess the possible role of larger scale horizontal advection (i.e. from outside of the eddy region) the near-surface circulation maps produced as hindcasts or analyses of the entire Mediterranean (MFSTEP, 2004) were examined. The maps provide daily, three-dimensional, gridded fields of temperature, salinity, and currents beginning from September 1999 that were produced through a four-dimensional data assimilation system. Throughout most of this period, the main data assimilated were satellite sea-surface temperature and height: hence, attention was focussed on the near-surface circulation, which is the most reliable. Upon comparing the late August-early September maps to the corresponding chl-a maps (Fig. 4) for the years 1999–2004, it was found that the location and shape of the high chl-a zone along the eastern edge of the domain, and the sharp separation between this zone and the lower concentration region to the west, closely follows the shelf/slope current position and the associate meanders. However there is no obvious correlation between the circulation and the potential advection or supply of chl-a from the west or from the south (along the coast of Sinai).

3.4. Primary production

Table 1 shows estimates of PP integrated to the 0.1% light level computed for the eddy centre from daily 9-km SeaWiFS data for seasonal cycles from September to August the following year. Average "yearly" integrated production was ~69 gC m^{-2} y^{-1}, with a variation from 84 gC m^{-2} y^{-1} in 1997–1998 to ~64 gC m^{-2} y^{-1} in 2001–2002 and 2002–2003. By comparison, Psarra et al. (2000) measured annual PP in the Cretan Sea shelf and slope regions of, respectively, 80 and 59 gC m^{-2} y^{-1}; the latter is more typical of the open-ocean results computed herein. Bosc et al. (2004) using essentially the same model computed annual production of 102–109 gC m^{-2} y^{-1} for the South Levantine Basin.

The long-term reduction in chl-a in the eddy centre (Fig. 5A) also is seen in the primary production although the change in PP from 1997–1998 to 2002–2003 is only ~25%. This is probably because the model predicts a sub-surface chl-a profile based on the surface C_{sat} value (Morel and Berthon, 1989), and as C_{sat} declines the surface waters become clearer, light penetrates deeper into the water column and so the productive layer becomes deeper.

These satellite retrievals are likely to be overestimates for a number of reasons. First, the light propagation component of the Morel (1991) model underestimates vertical light attenuation when compared to a full radiative transfer equation solution (Liu et al., 1999) and therefore overestimates PP (Smyth et al., 2005). For instance,

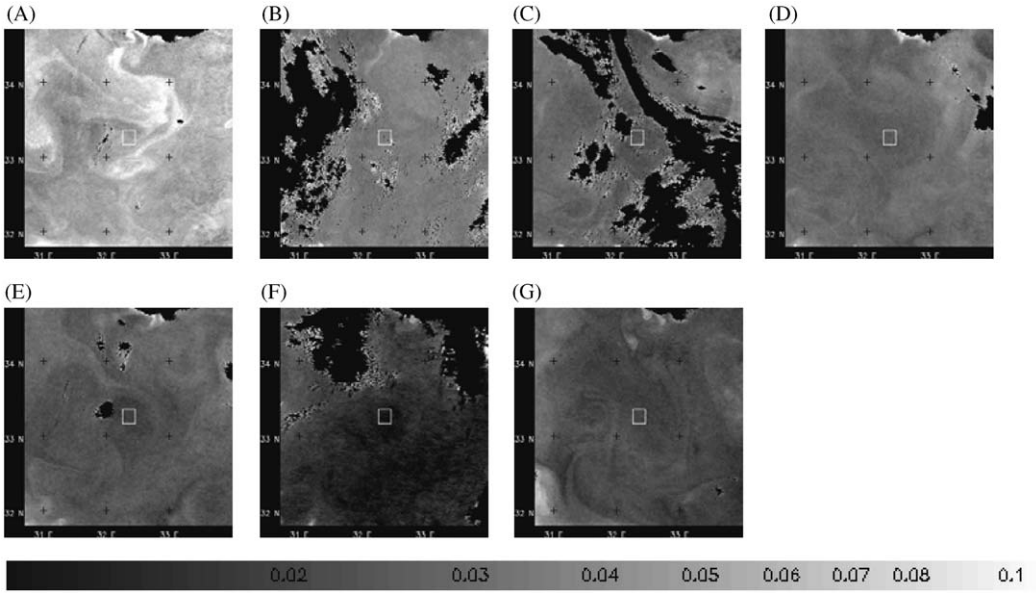

Fig. 8. Sequence of SeaWiFS chl-a images from Spring 2002: 10 April, 1, 18, 20, 25 May, 4 and 20 June with common contrast enhancement. Locations of the "eddy centre" box used for extraction in Fig. 9 are depicted.

the modelled primary production for 16 May 2002 is reduced by 10% using the improved in water light field. Second, the chl-a values used in the model are derived from the B2002 algorithm that has a residual overestimate of chl-a (by ~33%) at values $<0.04\,\mathrm{mg\,m^{-3}}$. Using reduced chl-a values reduces PP by ~8% overall during the year.

3.5. Chl-a variability in Spring 2002

The CYCLOPS phosphate-addition experiment was conducted in mid-May 2002, and daily SeaWiFS images were analysed from April to July to investigate chl-a variability around this period. Representative SeaWiFS passes are shown at full resolution in Fig. 8: the images have common contrast enhancement. The most noticeable feature of Fig. 8 is the decrease in chl-a throughout the sequence. This trend is quantified by computing average chl-a in a $0.2^\circ \times 0.2^\circ$ box around the eddy centre as measured during the cruises (see Law et al., 2005) and plotted in Fig. 9. The open squares represent all cloud-free pixels whilst the solid squares show only pixels that pass all 24 of the SeaWiFS quality criteria: on some days there are no pixels that pass all the criteria. Chl-a falls from $\sim 0.05\,\mathrm{mg\,m^{-3}}$ around 10 and 12 May (Julian days 100 and 102) to $\sim 0.03\,\mathrm{mg\,m^{-3}}$ by 29 Apr/1 May (days 119 and 121), and by the day of the phosphate release on 17 May had fallen to $\sim 0.02\,\mathrm{mg\,m^{-3}}$. The decline appears to continue to early June when chl-a was between $0.020\,\mathrm{mg\,m^{-3}}$ on 3 June and $0.012–0.013\,\mathrm{mg\,m^{-3}}$ on 4 and 7 June. Later chl-a was higher at 0.02 and $0.016\,\mathrm{mg\,m^{-3}}$ on 20 and 30 June, respectively.

The decrease in chl-a seen in Figs. 8 and 9 corresponds to the onset of summer oligotrophic conditions observed on the monthly plots in Fig. 4. Individual days such as 3 June appear to be higher than the general trend possibly as a result of atmospheric conditions such as absorbing aerosols affecting the SeaWiFS retrievals (Moulin et al., 2001). Scatter around the trend is obviously reduced by excluding data that have pixels with quality flags set. It is clear that the CYCLOPS addition experiment was conducted in a period of overall decrease in chl-a in the eddy. Considering only the data that pass all the exclusion criteria between 10 April and 7 June (days 100–158) there was a strong correlation between chlorophyll and day ($\mathrm{chl} = 0.00064\ \mathrm{day} + 0.112$; $r^2 = 0.91$), i.e. the long term decrease in chlorophyll within the study area represented an average decrease of $0.00064\,\mathrm{mg\,m^{-3}}$ per day.

One of the conclusions of the CYCLOPS 2002 cruise was that there was a small but statistically significant decrease in the observed chl-a following the phosphate addition (see other papers this volume and Thingstad et al., 2005). Specifically, Psarra et al. (2005) have compared in situ chl-a

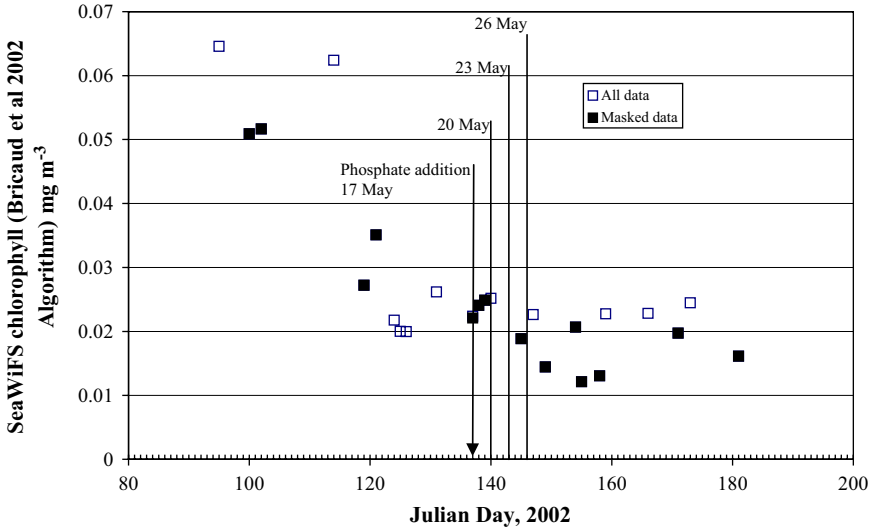

Fig. 9. Average chl-a at the eddy centre extracted from individual SeaWiFS images: open squares all cloud free pixels; filled squares exclude pixels that are masked by any of the 24 SeaWiFS quality flags.

estimates from HPLC and fluorometry (FL) and reported statistically significant differences between (a) the pre-addition (PRE) and post-addition stations inside (IN) the elevated phosphate patch for HPLC and (b) the PRE and stations outside (OUT) the elevated phosphate patch stations for FL. However, no significant differences were found for PRE/OUT and IN/OUT for HPLC and PRE/IN and IN/OUT for FL. Considering purely the statistically significant HPLC PRE/IN comparison, Psarra et al. (2005) report a decrease from $\sim 0.018\,mg\,m^{-3}$ just prior to the experiment to $0.011\,mg\,m^{-3}$ on day 5 (see their Fig. 4B) equal to an average reduction of $\sim 0.0014\,mg\,m^{-3}$ per day over the five days. This decrease is a factor of 2.2 greater than the average observed by SeaWiFS over the April–early June period.

An analysis like that that done in Psarra et al. (2005) is possible with SeaWiFS data since clear images were available from 17 May (day of the addition) 18, 19, 20 and 25 May (see Figs. 8 and 9). (Note that chl-a values on 20 May had the "moderate sunglint flag" set all over the region, but since there was no evidence that the sunglint is correlated with the eddy it was assumed that *differences* between the stations on 20 May would still be observable.) Chl-a variability on the day of the addition was computed for a manually selected region covering the southern half of the centre of the eddy, avoiding the cloud contamination over the northern part, and gave mean Chl-a $= 0.020\,mg\,m^{-3}$ with SD $= 0.0012$ both computed from 289 pixels.

However, before investigating remote sensing based statistical comparisons it is worth considering the accuracy of satellite retrievals. The RMSE of individual SeaWiFS retrievals as estimated by global in situ and satellite matchups is $\sim 0.23\log_{10}$ Chl-a (McClain et al., 2004) or from Fig. 2B $\sim 0.16\log_{10}$ Chl-a for the Bricaud et al. (2002) algorithm (equivalent to a range of 0.028–$0.058\,mg\,m^{-3}$ for a chlorophyll value of $0.04\,mg\,m^{-3}$). This contrasts with the lower variability observed in the eddy prior to the experiment (SD$\sim$0.0012). However, since the matchups are a test of the entire SeaWiFS system including the calibration, atmospheric correction and bio-optical algorithm, it is likely that day to day differences in atmospheric conditions or SeaWiFS viewing geometry will add variability to that observed within any one day.

Comparisons were first made between SeaWiFS chl-a values at IN and OUT stations on each of the two days (20 and 25 May), where clear SeaWiFS data were available and pairs of IN and OUT stations were sampled in situ (Psarra et al., 2005: Fig. 2A). On 20 May the chl-a at the IN and OUT stations (38 and 41, respectively) was for SeaWiFS 0.025 and $0.023\,mg\,m^{-3}$ compared to 0.016 and $0.013\,mg\,m^{-3}$ (FL) and 0.0127 and $0.0156\,mg\,m^{-3}$ (HPLC: Psarra et al., 2005). The higher SeaWiFS values were probably due to the moderate sunglint.

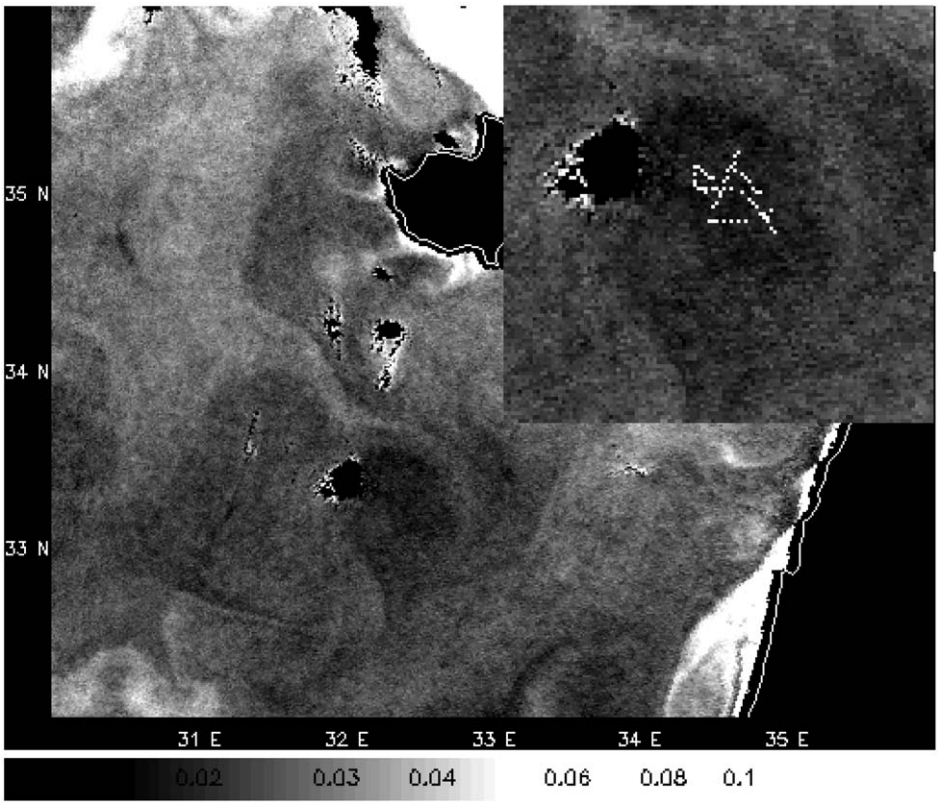

Fig. 10. SeaWiFS chlorophyll image for 25 May 2002 computed using Bricaud et al. (2002) algorithm. The inset shows positions of sampling locations on 25 and 26 May where SF_6 was above the operational threshold.

On 25 May the IN and OUT chl-a (at stations 62 and 64) were 0.021 and 0.018 mg m^{-3} (SeaWiFS), 0.018 and 0.019 mg m^{-3} (FL), 0.014 and 0.017 mg m^{-3} (HPLC). Hence, on both days SeaWiFS showed higher values *inside* the experiment. Assuming errors in retrievals are random, a 3×3 average around the location of each station would reduce errors, and differences were smaller than for individual pixels with values for IN/OUT stations of 0.024/0.025 mg m^{-3} for 20 May and 0.021/0.019 mg m^{-3} for 25 May. An alternative to comparisons at individual casts is to extract SeaWiFS chl-a values at each of the SF_6 sampling locations classified as IN and OUT using the operational threshold of 3 fmol l^{-1}. This enabled a much larger number of locations known to be inside or outside the experiment to be sampled from SeaWiFS. Fig. 10 shows, as an example, the SeaWiFS chl-a image for 25 May overlaid (in the inset) with the SF_6 "IN" locations from 25 and 26 May: it appears that the eddy has a very low chl-a core; however, the low values extend beyond the range of the "IN" locations. For 18 May there was a very small difference between IN (mean = 0.025 mg m^{-3}, SD = 0.005, $n = 67$) and OUT (mean = 0.024 mg m^{-3}, SD = 0.003, $n = 15$); on 20 May the mean IN and OUT chl-a were virtually identical at both stations (mean = 0.025 mg m^{-3}, SD$\sim$0.002); and on 25 May the IN value was marginally lower (0.0191 mg m^{-3}, SD = 0.0013, $n = 55$) than the OUT (0.0195 mg m^{-3}, SD = 0.0013, $n = 22$). However, none of the differences were statistically significant (using single tailed *t*-test) given the observed standard deviations. It may be questioned whether the number of points sampled is sufficient to detect a change: *if* the mean satellite-observed difference between IN and OUT values on 25 May was 0.001 mg m^{-3} (cf. observed in situ values of 0.001 mg m^{-3} for fluorometric and 0.003 mg m^{-3} for HPLC: Psarra et al., 2005 Fig. 3) with the same very low observed standard deviation (0.0013), the result would have been significant at the 0.5% level suggesting sample size was sufficient.

Finally, quantitative comparisons were first made between IN and OUT stations for 18 and 19 May and pre-addition conditions at the same locations on 17 May. Obviously, due to movement in the eddy, the water at a given location on 17 May was different to that on subsequent days; however, all water prior to the experiment was assumed to have similar nutrient status. Fig. 9 shows that average chl-a in the eddy-centre box exhibited a slight increase between 17 and 19 May. By contrast chl-a at both IN and OUT dropped between 17 and 18, but neither change was statistically significant. Average chl-a at IN stations on 19 May was identical to the same locations on 17 May whilst there were too few OUT stations for analysis.

4. Concluding remarks and future work

The CYCLOPS project investigated the impact of addition of phosphate on the microbial ecosystem in phosphate-limited waters in the ultra-oligotrophic Eastern Mediterranean. This paper investigated the seasonal and inter-annual variability in chl-a in the region with particular focus on the Cyprus Eddy, the location of the phosphate addition experiment in May 2002.

A database of chl-a measurements obtained on six cruises enabled comparison with satellite derived chl-a and confirmed the well known overestimation (Fig. 1C, D) inherent in using optical remote sensing algorithms in low chl-a waters in the Mediterranean. Satellite-in situ matchups (Fig. 2), though few in number, were primarily within the ultra-oligotrophic waters that previously had been relatively poorly sampled. The matchups showed a significant improvement in retrievals using the Bricaud et al. (2002) "regional" SeaWiFS algorithm. Although the SeaWiFS results were promising, there was a residual overestimation in chl-a at low values ($<0.04\,mg\,m^{-3}$). This suggests that a more comprehensive study is needed encompassing a wide range in chlorophyll values and atmospheric conditions to investigate whether there is seasonal or inter-annual variability in the chl-a retrievals. Furthermore, modified algorithms may be required for use with NASA's current MODIS ocean colour sensors: the MODIS matchups suggested that the chlor_a_3 algorithm is a promising candidate for future studies of chl-a in the Mediterranean. However, it should be stressed that these results are relevant to the earlier MODIS instrument on Terra (the only MODIS instrument available during the main CYCLOPS cruises); significant effort has been made by NASA to improve retrievals from the more recent MODIS on the Aqua platform.

The B2002 algorithm was used to compute SeaWiFS climatological monthly chl-a maps using data from Sept 1997 to August 2004 (Fig. 3) and presented as seven seasonal cycles from September to August the following year (Fig. 4). These showed a reduction in chl-a over the seven annual cycles of SeaWiFS data while average chl-a extracted using a quasi-Lagrangian approach from the centre of the Cyprus Eddy (Fig. 5A), as it moved westward, showed decreases in minima, maxima and average chl-a of ~33% between 1997–1998 and 2003–2004. It was hypothesized that the changes in chl-a were related to the dynamics of eddy, possibly as a result of limited winter vertical mixing in the core of this anticyclonic eddy (with a depressed nutricline), since no correlation was found with integrated heat flux (Fig. 6A), aerosol index (Fig. 6B) nor dust flux (as represented by annual Al flux measured on the Israeli coast, Fig. 7). Clearly the impact of dust deposition on the biology of surface waters and the satellite estimates of chl-a needs to be quantitatively evaluated at shorter timescales to match the duration of dust storms.

Finally, SeaWiFS data showed that the May 2002 phosphate addition was conducted in a period of decreasing chl-a as the surface nutrients became depleted with chl-a dropping from $\sim 0.05\,mg\,m^{-3}$ around 10 April to $0.013–0.02\,mg\,m^{-3}$ in late May and early June (Figs. 8 and 9). The average daily decrease over the this period was $\sim 0.00064\,mg\,m^{-3}$; by contrast the average daily decrease observed over five days in situ by Psarra et al. (2005) was $\sim 0.0014\,mg\,m^{-3}$. This suggests that the in situ decrease was not merely due to the longer-term chlorophyll decrease at the onset of nutrient limited oligotrophic conditions. Comparisons were made between SeaWiFS chl-a on individual days between locations known to be inside and outside the phosphate addition, but no statistically significant differences could be detected and so the small chl-a reduction observed in situ could not be observed using remote sensing.

Acknowledgements

This work was part funded by the EV Framework 5 CYCLOPS (Cycling of Phosphate in the Eastern Mediterranean Project (EVK3-CT-1999-00037) and by the Natural Environment Research Council core

support of Plymouth Marine Laboratory. We would like to acknowledge the masters and crew on the research vessels Aegaeo and Shikmona used to gather in situ data as well as CYCLOPS colleagues who under took cruise organisation and logistics (including Pre Carbo, Leeds University, and Anastasios Tselepides, HCMR Crete) and phosphate release/tracer and buoy operations (Malcolm Liddicoat and Tim Fileman, PML). We would like to thank Ben Wheatley, PML for running the primary production models and Bob Clarke, PML for statistical advice. We also thank staff at the Remote Sensing Data Analysis Service, Plymouth for assistance in satellite data processing and David Blondeau-Patissier for assistance in the MODIS/in situ comparisons. We acknowledge data provided by the NOAA-CIRES Climate Diagnostics Center, Boulder, Colorado, from their Web site at http://www.cdc.noaa.gov/. Finally, we would like to thank the reviewers Alex Cunningham and Peter Strutton and an anonymous reviewer for comments that improved the paper.

References

Antoine, D., Morel, A., Andre, H.M., 1995. Algal pigment distribution and primary production in the Eastern Mediterranean as derived from coastal zone color scanner observations. Journal of Geophysical Research 100, 16,193–16,209.

Baith, K., Lindsay, R., Fu, G., McClain, C.R., 2001. SeaDAS: data analysis system developed for ocean color satellite sensors. EOS, Transaction of the American Geophysical Union 82, 202–205.

Berman, T., Townsend, D.W., El-Sayed, S.Z., Trees, C.C., Azov, Y., 1984. Optical transparency, chl-a and primary productivity in the Eastern Mediterranean near the Israeli coast. Oceanologica Acta 7, 367–372.

Bethoux, J.P., Morin, C., Gentili, B., 1992. Phosphorous and nitrogen behaviour in the Mediterranean Sea. Deep-Sea Research 39, 1641–1654.

Bosc, E., Bricaud, A., Antoine, D., 2004. Seasonal and interannual variability in algal biomass and primary production in the Mediterranean Sea, as derived from 4 years of SeaWiFS observations. Global Biogeochemical Cycles 18, Art. no. GB1005.

Brenner, S., 1993. Long term evolution and dynamics of a persistent warm core eddy in the eastern Mediterranean. Deep-Sea Research II 40, 1193–1260.

Brenner, S., 2003. High-resolution nested model simulations of the climatological circulation in the southeastern Mediterranean Sea. Annals of Geophysics 21, 267–280.

Bricaud, A., Bosc, E., Antoine, D., 2002. Algal biomass and sea surface temperature in the Mediterranean basin: intercomparison of data from various satellite sensors, and implications for primary production estimates. Remote Sensing Environment 81, 163–178.

Carder, K.L., Chen, F.R., Lee, Z.P., Hawes, S., Kamykowski, D., 1999. Semi-analytic MODIS algorithms for chl-a and absorption with bio-optical domains based on nitrate-depletion temperatures. Journal of Geophysical Research 104, 5403–5421.

Claustre, H., Morel, A., Hooker, S.B., Babin, M., Antoine, D., Oubelkheir, K., Bricaud, A., Leblanc, K., Quéguiner, B., Maritorena, S., 2002. Is desert dust making oligotrophic waters greener? Geophysical Research Letters 29, 1469.

D'Ortenzio, F., Marullo, S., Ragni, M., Ribera d'Alcalà, M., Santoleri, R., 2002. Validation of empirical SeaWiFS algorithms for chl-a retrieval in the Mediterranean Sea: a case study for oligotrophic seas. Remote Sensing of Environment 82, 79–94.

D'Ortenzio, F., Ragni, M., Marullo, S., Ribera d'Alcalà, M., 2003. Did biological activity in the Ionian Sea change after the Eastern Mediterranean Transient? Results from the analysis of remote sensing observations. Journal of Geophysical Research 108, 8113–8132.

Esaias, W.E., Abbott, M.R., Barton, I., Brown, O.B., Campbell, J.W., Carder, K.L., Clark, D.K., Evans, R.H., Hoge, F.E., Gordon, H.R., Balch, W.M., Letelier, R., Minnett, P.J., 1998. An overview of MODIS capabilities for ocean science observations. IEEE Transactions on Geoscience and Remote Sensing 36, 1250–1265.

Gitelson, A., Karnieli, A., Goldman, N., Yacobi, Y.Z., Mayo, M., 1996. Chl-a estimation in the Southeastern Mediterranean using CZCS images: adaptation of an algorithm and its validation. Journal of Marine Systems 9, 283–290.

Gordon, H.R., Clark, D., 1980. Remote sensing optical properties of a stratified ocean: an improved interpretation. Applied Optics 19, 3428–3430.

Gregg, W.W., Carder, K.L., 1990. A simple spectral solar irradiance model for cloudless maritime atmospheres. Limnology and Oceanography 35, 1657–1675.

Herut, B., Krom, M.D., Pan, G., Mortimer, R., 1999. Atmospheric input of nitrogen and phosphorus to the Southeast Mediterranean: sources, fluxes, and possible impact. Limnology and Oceanography 44, 1683–1692.

Herut, B., Collier, R., Krom, M.D., 2002. The role of dust in supplying nitrogen and phosphorus to the Southeast Mediterranean. Limnology and Oceanography 47, 870–878.

Herut, B., Shefer, E., Cohen, Y., 2004. Quality of the coastal Mediterranean marine environment in Israel during 2003. IOLR Report H23/2004, H23a/2004—Executive summary in English, see www.ocean.org.il, (in Hebrew).

Hsu, N.V., Herman, J.R., Bhartia, P.K., Seftor, C.J., Torres, O., Thompson, A.M., Gleason, J.F., Eck, T.F., Holben, B.N., 1996. Detection of biomass burning smoke from TOMS measurements. Geophysical Research Letters 23, 745–748.

Joint, I., Groom, S.B., Wollast, R., Chou, L., Tilstone, G.H., Figueiras, F.G., Loijens, M., Smyth, T.J., 2002. The response of phytoplankton production to periodic upwelling and relaxation events at the Iberian shelf break: estimates by the C-14 method and by satellite remote sensing. Journal of Marine Systems 32, 219–238.

Karabashev, G., Evdoshenko, M., Sherberstov, S., 2002. Penetration of coastal waters into the Eastern Mediterranean Sea using SeaWiFS data. Oceanologica Acta 25, 31–38.

Krom, M.D., Kress, N., Brenner, S., Gordon, L.I., 1991. Phosphorus limitation of primary productivity in the Eastern Mediterranean. Limnology and Oceanography 36, 424–432.

Krom, M.D., Brenner, S., Kress, N., Neori, A., Gordon, L.I., 1993. Nutrient distributions during an annual cycle across a warm-core oceanic eddy from the E. Mediterranean Sea. Deep-Sea Research 40, 805–825.

Krom, M.D., Groom, S., Zohary, T., 2003a. The Eastern Mediterranean. In: Black, K.D., Shimmield, G.B. (Eds.), The Biogeochemistry of Marine Systems. Blackwell, Oxford, pp. 91–126.

Krom, M.D., Herut, B., Mantoura, R.F.C., 2003b. Nutrient budget for the Eastern Mediterranean: implications for phosphorus limitation. Limnology and Oceanography 49, 1582–1592.

Krom, M.D., Thingstad, T.F., Carbo, P., Drakopoulos, P., Fileman, T.W., Flaten, G.A.F., Groom, S., Herut, B., Kitidis, V., Kress, N., Law, C.S., Liddicoat, M.I., Mantoura, R.F.C., Pasternak, A., Pitta, P., Polychronaki, T., Psarra, S., Rassoulzadegan, F., Skjoldal, E.F., Spyres, G., Tanaka, T., Tselepides, A., Wassmann, P., Wexels-Riser, C., Woodward, E.M.S., Zodiatis, G., Zohary, T., 2005. Summary and overview of the CYCLOPS P addition Lagrangian experiment in the Eastern Mediterranean. Deep-Sea Research II, this issue [doi:10.1016/j.dsr2.2005.08.018].

Lavender, S.J., Groom, S.B., 1999. The SeaWiFS automatic data processing system, SeaAPS. International Journal of Remote Sensing 20, 1051–1056.

Law, C.S., Abraham, E.R., Woodward, E.M.S., Liddicoat, M.I., Fileman, T., Thingstad, T.F., Kitidis, V., Zohary, T., 2005. The fate of phosphate in an in situ Lagrangian addition experiment in the Eastern Mediterranean. Deep-Sea Research II, this issue [doi:10.1016/j.dsr2.2005.08.017].

Levitus, S., 1982. Climatological atlas of the world ocean, NOAA Prof. Paper, 13. Washington, DC, US Government Printing Office.

Liu, C.C., Woods, J.D., Mobley, C.D., 1999. Optical model for use in oceanic ecosystem models. Applied Optics 38, 4475–4485.

Mantoura, R.F.C., Llewellyn, C.A., 1983. The rapid determination of algal chl-a and carotenoid pigments and their breakdown products in natural waters by reverse-phase high-performance liquid chromatography. Analytica Chimica Acta 151, 297–314.

McClain, C.R., Feldman, G.C., Hooker, S.B., 2004. An overview of the SeaWiFS project and strategies for producing a climate research quality global ocean bio-optical time series. Deep-Sea Research II 51, 5–42.

MFSTEP, 2004. Mediterranean forecasting system, towards environmental prediction, WWW page, http://www.bo.ingv.it/mfstep.

Morel, A., 1991. Light and marine photosynthesis: a model with geochemical and climatological implications. Progress in Oceanography 26, 301–342.

Morel, A., Berthon, J.F., 1989. Surface pigments, algal biomass profiles, and potential production of the euphotic layer: relationship reinvestigated in view of remote-sensing applications. Limnology and Oceanography 34, 1545–1562.

Morel, A., Antoine, D., Babin, M., Dandonneau, Y., 1996. Measured as modelled primary production in the northeast Atlantic, EUMELI JGFS program: the impact of natural variations in photosynthetic parameters on model predictive skill. Deep-Sea Research I 43, 1273–1304.

Moulin, C., Gordon, H.R., Chomko, R.M., Banzon, V.F., Evans, R.H., 2001. Atmospheric correction of ocean color imagery through thick layers of Saharan dust. Geophysical Research Letters 28, 5–8.

O'Reilly, J.E., Maritorena, S., Mitchell, B.G., Siegel, D.A., Carder, K.L., Garver, S.A., Kahru, M., McClain, C., 1998. Ocean color chl-a algorithms for SeaWiFS. Journal of Geophysical Research 103, 24937–24953.

Ozsoy, E., Hect, A., Unluata, U., Brenner, S., Sur, H.I., Bishop, J., Oguz, T., Rosentraub, Z., Latif, M.A., 1993. A synthesis of the Levantine basin circulation and hydrography, 1985–1990. Deep Sea Research II 40, 1075–1119.

Prieur, L., Sathyendranath, S., 1981. An optical classification of coastal and oceanic waters based on the specific spectral absorption curves of phytoplankton pigments, dissolved organic-matter, and other particulate materials. Limnology and Oceanography 26, 671–689.

Psarra, S., Tselepides, A., Ignatiades, L., 2000. Primary productivity in the oligotrophic Cretan Sea, NE Mediterranean: seasonal and interannual variability. Progress in Oceanography 46, 187–204.

Psarra, S., Zohary, T., Krom, M.D., Mantoura, R.F.C., Polychronaki, T., Stambler, N., Tanaka, T., Tselepides, A., Thingstad, T.F., 2005. Phytoplankton response to a Lagrangian phosphate addition in the Levantine Sea (Eastern Mediterranean). Deep-Sea Research II, this issue [doi:10.1016/j.dsr2.2005.08.015].

Reynolds, R.W., Smith, T.M., 1995. A high-resolution global sea surface temperature climatology. Journal of Climate 8, 1571–1583.

Siegel, D.A., Wang, M.H., Maritorena, S., Robinson, W., 2000. Atmospheric correction of satellite ocean color imagery: the black pixel assumption. Applied Optics 39, 3582–3591.

Smyth, T.J., Tilstone, G.H., Groom, S.B., 2005. Integration of radiative transfer into satellite models of ocean primary production. Journal of Geophysical Research 110, C10014, doi:10.1029/2004JC002784.

Stratford, K., Haines, K., 2002. Modelling nutrient cycling during the Eastern Mediterranean Transient event 1987–1995 and beyond. Geophysical Research Letters 29, 1–4.

Thingstad, T.F., Krom, M.D., Mantoura, R.F.C., Flaten, G.A.F., Groom, S., Herut, B., Kress, N., Law, C.S., Pasternak, A., Pitta, P., Psarra, S., Rassoulzadegan, F., Tanaka, T., Tselepides, A., Wassmann, P., Woodward, E.M.S., Wexels Riser, C., Zodiatis, G., Zohary, T., 2005. Nature of phosphate limitation in the oligotrophic Eastern Mediterranean. Science 309, 1068–1071.

Turley, C.M., Bianchi, M., Christaki, U., Conan, P., Harris, J.R.W., Psarra, S., Ruddy, G., Stutt, E.D., Tselepides, A., Van Wambeke, F., 2000. Relationship between primary producers and bacteria in an oligotrophic sea—the Mediterranean and biogeochemical implications. Marine Ecology Progress Series 193, 11–18.

Yacobi, Y.Z., Zohary, T., Kress, N., Hecht, A., Robarts, R.D., Waiser, M., Wood, A.M., Li, W.K.W., 1994. Chlorophyll distribution throughout the southeastern Mediterranean in relation to the physical structure of the water mass. Journal of Marine Systems 6, 179–190.

Yentsch, C.S., Menzel, G.L., 1963. A method for the determination of phytoplankton chl-a and phaeophytin by fluorescence. Deep-Sea Research 10, 221–231.

Zodiatis, G., Bruno, M., Balopoulos, E., 2001. Synoptic, seasonal and interannual variability of the warm Core Eddy south of Cyprus, SE Levantine Basin. Rapport du Commission

Internationale pour l'Exploration Scientifique de la Mer Méditerranée 36, 89.

Zodiatis, G., Drakopoulos, P., Brenner, S., Groom, S., 2002. CYCLOPS project: the hydrodynamics of the warm Core Eddy south of Cyprus. Second International Conference: Oceanography of the Eastern Mediterranean and Black Sea, October, Ankara.

Zodiatis, G., Drakopoulos, P., Gertman, I., 2004. Modified Atlantic water in the SE Levantine Basin, 1995–2003. Rapport du Commission Internationale pour l'Exploration Scientifique de la Mer Méditerranée 37, 156.

Zodiatis, G., Drakopoulos, P., Brenner, S., Groom, S., 2005. Variability of the Cyprus warm Core Eddy during the CYCLOPS project, this volume.

Zohary, T., Brenner, S., Krom, M.D., Angel, D.L., Kress, N., Li, W.K.W., Neori, A., Yacobi, Y.Z., 1998. Build-up of microbial biomass during deep winter mixing in a Mediterranean warm-core Eddy. Marine Ecology Progress Series 167, 47–57.